EPJ Web of Conferences **17**, 09005 (2011)
DOI: 10.1051/epjconf/20111709005

Investigation of fission properties and evaporation residue measurement in the reactions using ^{238}U target nucleus

K. Nishio[1,a], H. Ikezoe[1], S. Hofmann[2,3], D. Ackermann[2], S. Antalic[4], Y. Aritomo[1,5], V.F. Comas[2,6], Ch.E. Düllmann[2], A. Gorshkov[7], R. Graeger[7], K. Hagino[8], S. Heinz[2], J.A. Heredia[2], K. Hirose[1,9], J. Khuyagbaatar[2], B. Kindler[2], I. Kojouharov[2], B. Lommel[2], H. Makii[1], R. Mann[2], S. Mitsuoka[1], Y. Nagame[1], I. Nishinaka[1], T. Ohtsuki[9], A.G. Popeko[5], S. Saro[4], M. Schädel[2], A. Türler[7], Y. Wakabayashi[1], Y. Watanabe[10], A. Yakushev[7], and A.V. Yeremin[5]

[1] Japan Atomic Energy Agency, Tokai, Ibaraki 319-1195, Japan
[2] GSI Helmholtzzentrum für Schwerionenforschung, 64291 Darmstadt, Germany
[3] Institut für Kernphysik, Goethe-Universität Frankfurt, 60438 Frankfurt am Main, Germany
[4] Department of Nuclear Physics and Biophysics, Comenius University, 84248 Bratislava, Slovakia
[5] Flerov Laboratory of Nuclear Reactions, 141 980 Dubna, Russia
[6] Higher Institute of Technologies and Applied Sciences, Habana 10400, Cuba
[7] Institut für Radiochemie, Technische Universität München, 85748 Garching, Germany
[8] Department of Physics, Tohoku University, Sendai 980-8597, Japan
[9] Laboratory of Nuclear Science, Tohoku University, Sendai 982-0826, Japan
[10] High Energy Accelerator Organization (KEK), Tsukuba 305-0801, Japan

Abstract. Fragment mass distributions for fission after full momentum transfer were measured in the reactions of ^{30}Si,^{34,36}S,^{31}P,^{40}Ar + ^{238}U at bombarding energies around the Coulomb barrier. Mass distributions change significantly as a function of incident beam energy. The asymmetric fission probability increases at sub-barrier energy. The phenomenon is interpreted as an enhanced quasifission probability owing to orientation effects on fusion and/or quasifission. The evaporation residue (ER) cross sections were measured in the reactions of ^{30}Si + ^{238}U and ^{34}S + ^{238}U to obtain information on fusion. In the latter reaction, significant suppression of fusion was implied. This suggests that fission events different from compound nucleus are included in the mass-symmetric fragments. The results are supported by a model calculation based on a dynamical calculation using Langevin equation, in which the mass distribution for fusion-fission and quasifission fragments are separately determined.

1 Introduction

Experiments to produce superheavy nuclei (SHN) have been carried out by using heavy ion fusion reactions [1–3]. Development of a theoretical model to predict cross sections for nuclei located at the extreme end of heavy elements is important for the proper selection of target and projectile as well as the bombarding energy to produce these nuclei. The reaction is considered to proceed in three steps; (1) penetration of the Coulomb barrier between two colliding nuclei, (2) formation of a compound nucleus after the system is captured inside the Coulomb barrier and (3) survival of the excited compound nucleus to produce evaporation residue (ER) against fission (fusion-fission).

The first step, penetrating the Coulomb barrier, is relatively well understood. Enhancing of the capture cross section ($\sigma_{\rm cap}$) relative to the one-dimensional barrier penetration model has been observed at sub-barrier energies. In a reaction involving deformed target nucleus, couplings to the rotational bands in a target nucleus is a major reason for enhancing the $\sigma_{\rm cap}$. The second process, forming a compound nucleus (fusion probability), is not well understood. A theoretical model must treat the dynamic evolution of a system from the initial touching configuration up to the so called compound nucleus state. In a reaction using a heavy target and projectile, quasifission competes against fusion. The cross section to produce SHN is then calculated from the fusion cross section by multiplying the survival probability by using a statistical model.

The ER cross section gives information on the fusion probability. However, because of the low production rate for SHN, available data with high statistical accuracy are limited. When a model can treat fusion-fission and quasifission in a consistent framework, such as the unified theory [4], the measurement of fission properties can be another benchmark for testing the model, as fusion-fission and quasifission would have different decay properties.

Fusion reactions using actinide target nuclei are extensively used to investigate SHN [1]. The accurate prediction of the cross sections for actinide-based reactions is important to explore this field. The prolate deformation of actinide nucleus should influence the fusion process. We

[a] e-mail: nishio.katsuhisa@jaea.go.jp

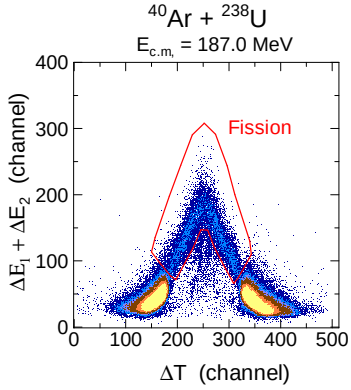

Fig. 1. Coincidence events plotted on ΔT and $\Delta E_1 + \Delta E_2$ in the reaction of ^{40}Ar+^{238}U.

have investigated the effects of nuclear orientation on fusion and/or quasifission by measuring the fission fragment mass distributions in the reactions using ^{238}U target nucleus. We also measured the ER cross sections as a direct evidence for fusion to confirm the validity of the fusion probability obtained from fission measurement.

2 Experimental details

2.1 In-beam fission measurement

The mass distributions and cross sections of fission fragments in the reactions of ^{30}Si,^{34,36}S,^{31}P,^{40}Ar + ^{238}U were measured using beams supplied by the tandem accelerator of the Japan Atomic Energy Agency (JAEA) in Tokai, Japan. The experimental set-up and the analysis method were described in [5].

Beam energies were changed from above-barrier to subbarrier values. The beam intensities were typically from 0.1 to 1.0 p-nA. The ^{238}U target was prepared by electrodeposition of UO_2 on a 90-μg/cm^2 thick nickel backing. Both fission fragments (FFs) were detected in coincidence by position-sensitive multiwire proportional counters (MWPCs). By using the position information, emission angles of both fission fragments were determined.

The time difference, ΔT, between the signals from MWPC1 and MWPC2 was measured. The charges induced in both MWPCs contain information on the energy deposition ΔE_1 and ΔE_2 of particles traversing the detectors and were recorded. In the two dimensional spectrum of ΔT versus $\Delta E_1 + \Delta E_2$ (Fig.1), fission events were well separated from elastically scattered projectile-target events.

In the data anysis, fission events occurring after complete transfer of the projectile momentum (full momentum transfer (FMT) fission) were used. These events were separated from events originating from nuclear transfer by measuring the folding angle between two fragments.

2.2 Evaporation residue measurement

Measurements of ER cross sections were carried out in the reactions of ^{30}Si + ^{238}U and ^{34}S + ^{238}U. The experiments

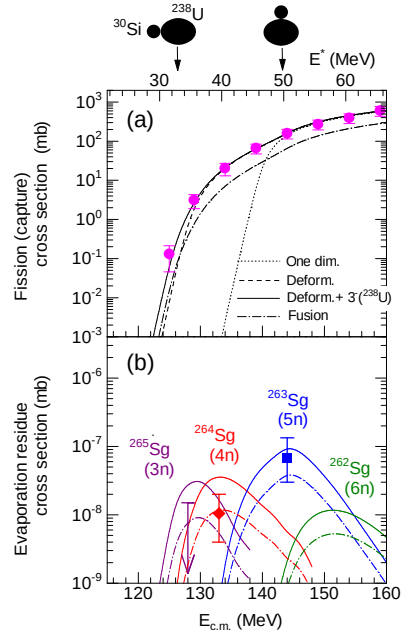

Fig. 2. (a) Excitation function for FMT fission and (b) evaporation residue cross sections for ^{30}Si + ^{238}U. Curves are the model calculations (see text)

were performed at the linear accelerator UNILAC and the velocity filter SHIP at GSI in Darmstadt. The SHIP set-up was essentially the same as described in [2]. Average beam intensities at the target position were typically 0.7−1.0 $p\mu$A for ^{30}Si and 2.0−2.5 $p\mu$A for ^{34}S. Details of the experiments are described in [6,7]. The uranium targets were prepared by evaporation of isotopically depleted $^{238}UF_4$ (^{30}Si +^{238}U run) or sputtering the depleted ^{238}U metal (^{34}S + ^{238}U run) on a carbon backing.

In the focal plane of the SHIP, ERs and their subsequent α decay and/or spontaneous fission (sf) were detected by a position sensitive 16-strip Si PIPS detector. The correlated events is identified primarily based on a coincidence of the positions of implanted ER, subsequent α decays and/or sf.

3 Experimental results

The cross section for the FMT fissions ($\sigma_{\rm fiss}$) of ^{30}Si + ^{238}U are shown in Fig.2(a) as a function of the center-of-mass energy, $E_{\rm c.m.}$, as well as a function of excitation energy of the compound nucleus, E^*. The fission cross section is almost equal to the capture cross section ($\sigma_{\rm cap}$).

The measured cross sections for ^{263,264}Sg and the upper limit value for ^{265}Sg in the fusion-evaporation reaction of ^{30}Si + ^{238}U [6] are shown in Fig.2(b).

In order to see the effects of nuclear properties on the capture cross sections, we show in Fig. 2(a) the calculation using the coupled-channels code, CCDEGEN [8]. The dotted curve is the result without considering any collective properties or deformation of the target and projectile (one-dimensional barrier penetration model). The Coulomb barrier V_B is 139.7 MeV. The dashed curve is the result which

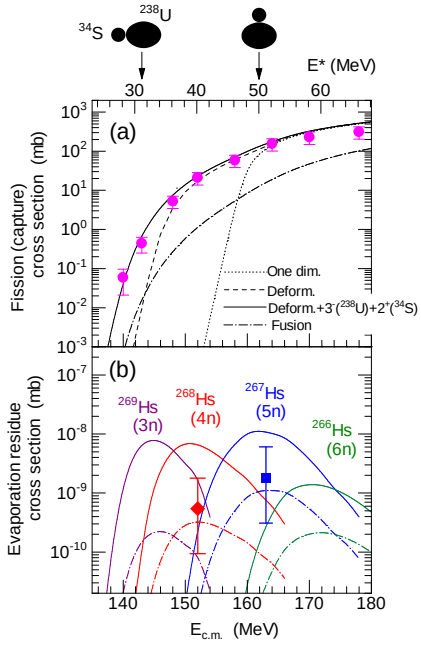

Fig. 3. (a) Excitation function for FMT fission and (b) evaporation residue cross sections for $^{34}S + ^{238}U$. Curves are the model calculations (see text).

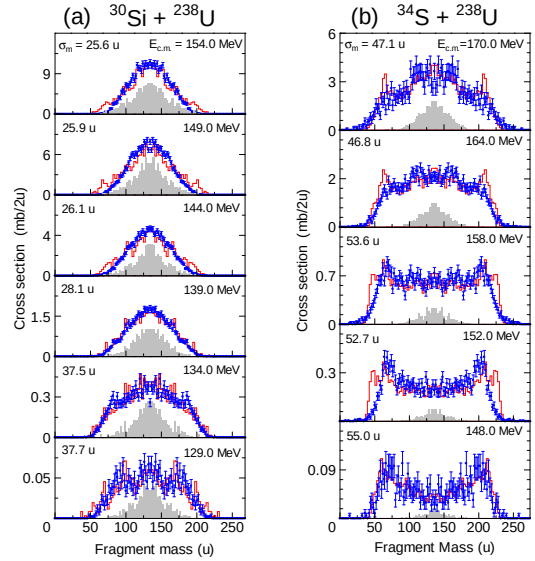

Fig. 4. Fragment mass distributions for FMT fissions of the reactions (a) $^{30}Si + ^{238}U$ and (b) $^{34}S + ^{238}U$. The experimental data are shown as dots. Histograms shows a model calculation. The calculated fusion-fission spectrum is shown by the filled area. Reaction energy in the center-of-mass system and the standard deviation σ_m of the measured spectrum are shown.

takes into account the prolate deformation of ^{238}U with $(\beta_2, \beta_4) = (0.275, 0.050)$ [9]. Low Coulomb barrier for the polar collisions, as sketched in the upper part of Fig. 2, is the main reason for enhancing the capture cross section in the sub-barrier reaction. The lowest energy data is, however, reproduced by additionally taking into account the coupling to the 3^- state at 0.73 MeV in ^{238}U [10] (β_3 =0.086 [11]), as shown by the solid curves.

The fission cross sections for $^{34}S + ^{238}U$ are shown in Fig. 3(a). The data are compared with the coupled-channels calculations. The assumptions given to draw the dotted and dashed curves are the same as in Fig.2(a). The V_B value is 159.1 MeV. The solid curve is the results which takes into account the couplings to the 3^- state (0.73 MeV) in ^{238}U and to the 2^+ state (2.13 MeV [10]) in ^{34}S (β_2 =0.25 [12]). The calculation reproduces the data down to the lowest beam energy.

The measured cross sections for ^{267,268}Hs in the fusion-evaporation reaction of $^{34}S + ^{238}U$ [7] are shown in Fig.3(b).

Figure 4(a) shows the mass distributions in the $^{30}Si + ^{238}U$ reaction. The yield is scaled by the cross section under the assumption that the mass distribution does not depend on $\theta_{c.m.}$. The distributions are Gaussian-shaped and centered at half of the mass of the composite system in the energy range from $E_{c.m.}$ = 139.0 MeV to 154.0 MeV. At the sub-barrier energy of $E_{c.m.}$ = 134.0 and 129.0 MeV, an asymmetric component around $A_L/A_H \approx 90/178$ appears. The difference of the mass distribution at the lowest energy data is characterized also by the standard deviation σ_m as indicated in each panel of Fig. 4(a). Considering the measured ER cross sections (Fig. 2(b)), as discussed in the following, we conclude that the asymmetric fission channel originates from quasifission.

The mass distributions in the $^{34}S + ^{238}U$ reaction are shown in Fig. 4(b). At the highest energy of 170.0 MeV, the distribution is Gaussian-shaped. The σ_m value of the spectrum, however, is larger than the value for $^{30}Si + ^{238}U$ at $E_{c.m.}$ =154.0 MeV. Towards the low incident energy, the asymmetric fission yield increases sharply around the mass asymmetry $A_L = 68$ and $A_H = 204$. This corresponds to the fragments near the double-closed shell nuclei, ^{78}Ni and ^{208}Pb [13]. The phenomenon was interpreted by the effects of nuclear orientation on fusion and/or quasifission. At the sub-barrier energy, projectiles collide only on the polar sides of the ^{238}U nucleus. In this case the reaction starts from a distant contact point with a large charge-center distance, which results in a larger quasifission probability than the reactions starting from the equatorial collisions.

Figure 5 shows the mass distributions in the reactions using different projectiles of ^{30}Si,^{31}P,^{36}S and ^{40}Ar. At a fixed excitation energy E*, a yield for an asymmetric fission channel increases with projectile charge, showing that quasifission probability increases due to larger Coulomb repulsive force in the reaction process. The enhanced quasifission yield toward the low incident energy are observed for all the reactions owing to the orientation effects.

4 Discussions

For a quantitative analysis of the mass distributions, we performed a model calculation combining the coupled channels method and a dynamical description of the reaction based on the three-dimensional Langevin equation [14]. The dynamical calculation based on the Monte Carlo method was used for describing the reaction paths in the potential

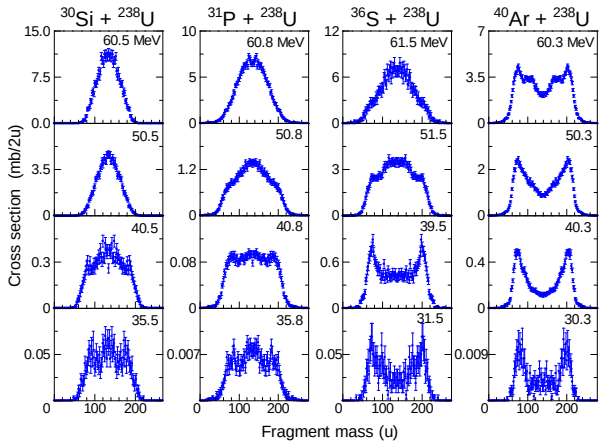

Fig. 5. Fission fragment mass distributions in the reactions of ^{30}Si,^{31}P,^{36}S,^{40}Ar + ^{238}U. The excitation energy E^* of a compound nucleus is shown in each spectrum.

energy landscape. The two-center shell model was used to calculate the potential energy of a nucleus. The deformation of the reaction partners and their orientation in the reaction plane was considered. Fusion is defined as the case when the trajectory enters inside the local energy minimum corresponding to the compound nucleus, whereas quasifission is defined as disintegration without reaching the minimum.

The calculated distributions of FMT fragments for ^{30}Si + ^{238}U are represented by the histograms in Fig. 4(a). The model reproduces the general shape of the distribution. The calculated fusion-fission events in this model are shown by the filled areas in Fig. 4(a). It is Gaussian-shaped, and the standard deviation of the spectrum $\sigma_{\rm m}$ is nearly constant with 21∼25 u in the entire energy range. The value is significantly smaller than 37 ∼ 38 u for the measured distributions at the sub-barrier energies of 129.0 and 134.0 MeV. Furthermore the calculated fusion-fission spectrum does not show any asymmetric fission channels. The results support the observed asymmetric fission to be quasifission. In the calculation, we determined the fusion probability $P_{\rm fus}$ as the ratio of fusion-fission events to the FMT fission events. By multiplying the $P_{\rm fus}$ to capture cross section ($\sigma_{\rm cap}$), a fusion cross section $\sigma_{\rm fus}$ is obtained. The results for ^{30}Si + ^{238}U are shown by the dash-dotted curve in Fig. 2(a).

The same calculation was made in the ^{34}S + ^{238}U reaction as shown in Fig. 4(b). The results reproduce the measured distribution, especially transition from symmetric to asymmetric mass distributions with different incident energy is well reproduced. The $\sigma_{\rm m}$ value in the calculated fusion-fission spectrum is 16−20 u, which is nearly the same as the ^{30}Si + ^{238}U reaction. The value is about factor two less than those for the measured distribution. A remarkable difference between ^{30}Si + ^{238}U and ^{34}S + ^{238}U reactions is the fusion-fission yield among the FMT fissions. Even in the symmetric mass region, the yield drops significantly in the case of ^{34}S projectile. The mass-symmetric fission in ^{34}S + ^{238}U include quasifission. It can be interpreted by a deep quasifission [4] that the trajectory approaches the shape more closer to the compound nucleus state than the quasifission which leads to the Pb/Ni-like nuclei. The fusion cross sections $\sigma_{\rm fus}$ for ^{34}S + ^{238}U are shown in Fig. 3(a) by the dash-dotted curve.

To see if the above model is appropriate to estimate the fusion probability, $P_{\rm fus}$, a statistical model code HIVAP [15] was used to calculate the ER cross sections by inputting the fusion cross sections for ^{30}Si + ^{238}U (dash-dotted curve in Fig. 2(a)), and the results are compared with the experimental data in Fig.2(b). The calculation reproduces the cross sections for ^{263,264}Sg within errors as well as the cross section limit for ^{265}Sg. Similarly, the model can account for the cross sections for ^{267,268}Hs produced in the fusion of ^{34}S + ^{238}U as shown in Fig. 3(b). If we assume all the fragments were arising from the compound nucleus fission, the ER cross sections would have values shown by the solid curves in Fig. 2(b) or Fig. 3(b). Apparently, this assumption conflicts the cross sections of ^{264,265}Sg and ^{267,268}Hs. Our calculation for fusion cross section, determined from the measured mass distribution and the fluctuation-dissipation model, accounts for the ER cross sections. In spite of the reduced fusion probability at sub-barrier energies, the calculated ER cross section in Fig. 2(b) and Fig. 3(b) reveal a yield to produce relatively neutron rich nuclei, when targets of deformed actinide nuclei are used. In addition to the 4n channel, the ERs from 3n-evaporation is possible to produce in deep sub-barrier energy.

We would like to thank the UNILAC staff and the crew of the JAEA tandem accelerator facility for preparation and operation of the beams. This work was supported by a Grant-in-Aid for Scientific Research of the Japan Society for the Promotion of Science.

References

1. Yu.Ts. Oganessian, J. Phys. G **34**, R165 (2007).
2. S. Hofmann and G. Münzenberg, Rev. Mod. Phys. **72**, 733 (2000).
3. K. Morita *et al.*, J. Phys. Soc. Jpn. **76**, 045001 (2007).
4. V. Zagrebaev and W. Greiner, J. Phys. G, **31** 825 (2005).
5. K. Nishio *et al.*, Phys. Rev. C **77**, 064607 (2008).
6. K. Nishio *et al.*, Eur. Phys. J. A **29**, 281 (2006).
7. K. Nishio *et al*,. Phys. Rev. C, **82** 024611 (2010).
8. modified version of the CCFULL code, K. Hagino *et al.*, Computer Phys. Comm. **123**, 143 (1999).
9. D.J. Hinde *et al*,. Phys. Rev. Lett, **74** 1295 (1995).
10. R.B. Firestone *et al*,. *Table of Isotopes Eighth Edition* (JohnWiley & Sons, Inc.)
11. R.H. Spear *et al.*, At. Data Nucl. Data Tables, **42**, 55 (1989).
12. S. Raman *et al.*, At. Data Nucl. Data Tables, **36**, 1 (1987).
13. M.G. Itkis *et al.*, Nucl. Phys. **A787**, 150c (2007).
14. Y. Aritomo, to be submitted.
15. W. Reisdorf and M. Schädel, Z. Phys. A **343**, 47 (1992).